http://app.pan.pl/SOM/app66-Klein_Surmik_SOM.pdf

SUPPLEMENTARY ONLINE MATERIAL FOR

Bone histology of *Proneusticosaurus* (Diapsida, Eosauropterygia) from the Middle Triassic of Poland reveals new insights into taxonomic affinities

Nicole Klein and Dawid Surmik

Published in *Acta Palaeontologica Polonica* 2021 66 (3): 585-598.
https://doi.org/10.4202/app.00850.2020

Supplementary Online Material

SOM Text. Histological description of eosauropterygian femora for comparison
SOM Table 1. Femora of Eosauropterygia histologically studied.
SOM Fig. S1. Microanatomy of femora of *Proneusticosaurus silesiacus* (MGU Wr. 4438s), the pachypleurosaurs *Neusticosaurus* and *Anarosaurus,* the nothosaur *Nothosaurus* spp. and of several femora Eosauropterygia indet.
SOM Fig. S2. Bone tissue, vascularization, and growth pattern in the pachypleurosaurs aff. *Neusticosaurus* and *Anarosaurus heterodontus*.
SOM Fig. S3. Bone tissue, vascularization, and growth pattern in femora of large *Nothosaurus* spp.
SOM Fig. S4. Bone tissue, vascularization, and growth pattern in Eosauropterygia indet. femora (most likely referable to *Nothosaurus* sp.).
SOM Fig. S5. Bone tissue, vascularization, and growth pattern in Eosauropterygia indet. femora.
SOM Fig. S6. Articulated vertebrae and ribs from the trunk region of *Nothosaurus* sp.
SOM Fig. S7. Ischia and pubes of *Proneusticosaurus* from varies Lower Muschelkalk localities.

Supplementary material

Supplementary Text

Histological description of eosauropterygian femora for comparison

Histological, microanatomy and growth pattern of femora of the pachypleurosaur aff. *Neusticosaurus* from the Ladinian of the Germanic Basin.—The medullary cavity in femora of aff. *Neusticosaurus* from Kirchheim is largely filled by endosteal bone. Periosteal resorption and remodelling are not visible. Femora consist of low vascularized (Suppl. Fig. S2A-D) highly organized parallel-fibred tissue and nearly avascular lamellar tissue (Suppl. Fig. S2A-D) in adult individuals. If present at all, vascular canals occur as longitudinal primary osteons and few simple radial vascular canals. Bone compactness in femora of aff. *Neusticosaurus* ranges from 89% to 99% (Table 1), resulting in osteosclerotic bones. Osteosclerosis is achieved by a thick compact cortex and endosteal remodelling.
Two out of the four femur samples show a less organized and well vascularized tissue in the inner half of the section (Suppl. Fig. S2A, B), most likely representing the tissue of the juvenile individual. This juvenile tissue is separated from the following cortex by an annulus and a LAG. The outer cortex consists of high organized and nearly avascular tissue that is stratified by LAGs. The other two samples do not show an inner ring of juvenile tissue. They are in general lower vascularized and more regularly stratified by LAGs throughout the entire cortex (Suppl. Fig. S2C, D). If this difference in growth pattern is related to sexual dimorphism or has taxonomical reasons cannot be clarified due to the small sample size.

Histological, microanatomy and growth pattern of femora of the pachypleurosaur *Anarosaurus heterodontus* from the middle Anisian.—Femora of *Anarosaurus heterodontus* show a moderately-sized free medullary cavity, which is lined by a thin layer of endosteal bone. This tissue is characterized by a relatively high vascular density, loosely organized parallel-fibred tissue, locally even intermixed with woven bone (Suppl. Fig. S2E-J). Primary osteons or at least partially lined simple vascular canals together with woven bone result in incipient fibro-lamellar bone (Klein 2010), that indicates high growth rates. Vascular canal orientation is mainly radial (Suppl. Fig. S2E-J).

In most samples of *Anarosaurus* no distinct (i.e. annual) growth marks are visible (Wijk07-11, Wijk06-38, Wijk06-266, Wijk fe I, Wijk06-84, WijkA565). Locally, subcycles in form of thin layers of highly organized tissue occur but cannot be followed all around the cross section (Suppl. Fig. S2F). In femur samples Wijk09-582 and Wijk07-11, a distinct annulus accompanied by a LAG is visible in the outer cortex (Suppl. Fig. S2I, J). Again, it cannot be clarified if this is related to sexual dimorphism or taxonomical differences. Because Wijk07-11 is a very small sized femur (Table 1), ontogenetic differences can be excluded.

Tissue type of *Anarosaurus heterodontus* femora represent a fast-growing tissue. It cannot be excluded that a similar tissue can occur in juvenile individuals of other eosauropterygian taxa such as *Nothosaurus* and basal pistosauroids and that some femora that are assigned to *Anarosaurus* in fact belong to another taxon. Femora here assigned to *Anarosaurus* have a range in bone compactness from 75% to 87% and are much less osteosclerotic when compared to other pachypleurosaurs or *Proneusticosaurus* (Table 1).

Histological, microanatomy and growth pattern of femora of large *Nothosaurus* spp. from the Ladinian.—Femora of large nothosaurs show a wide spectrum of differently organized parallel-fibred tissue in some samples grading into lamellar tissue and vascularization (i.e. density and organization) (Suppl. Fig. S3). Canal orientation is mainly longitudinal and radial, primary osteons and simple vascular canals can occur in the same sample (Suppl. Fig. S3). Periosteal resorption as well as endosteal remodelling can occur. The size of the medullary cavity and/or region varies greatly from small reduced (SMNS 84844, SMNS 59373, SMNS 84856, MHI 1992, SMNS 81883, SMNS 81886), over moderately sized (IGPB R 54, MHI 1987, MHI 756, SMNS Weismann Nr 79, IGPB R 50, MHI 2011), a large spongious medullary region (MHI 1113; SMNS 5308, IPGB R 49) to large cavities (SMNS Knapp 1869, MHI 279) (Table 1; Suppl. Fig. S1). Mirroring this diversity, bone compactness values vary between 57.6% and 96%. Osteosclerosis is achieved either by a small reduced cavity or by endosteal remodeling/deposits. Bone mass decrease is achieved by the presence of large medullary cavities or periosteal resorption. All nothosaurs show growth marks in form of sequential appearing zones, annuli and LAGs. In some samples, growth marks are only diffuse (Suppl. Fig. S3C-E), in other they are very clear and regularly (Suppl. Fig. S3F, H. I) or irregularly spaced (Suppl. Fig. S3B, G).

Histological and microanatomical description of small to medium sized eosauropterygian femora from the early to middle Anisian.—Several femora, which cannot undoubtedly be assigned to a certain taxon (neither based on morphology nor on histology), show a tissue dominated by differently organized parallel-fibred bone with a low to moderate vascular density (Suppl. Fig. S4, 5), except for Wijk06-86 (Suppl. Fig. S5C, D) and TWE 48000085 (Suppl. Fig. S5A, B) where vascular density is high. Canal orientation is mainly a mixture of longitudinal and radial ones, except for IGWH 24 (Suppl. Fig. S5E, F) where the entire cross section displays only longitudinal primary osteons and some others where a radial orientation dominates (e.g., Wijk06-14, Fig. 7G, H, TWE 48000085, Suppl. Fig. S5A, B). Usually, primary osteons and simple vascular canals can occur in the same sample. Periosteal resorption is rare whereas endosteal remodelling occurs more often.

The size of the medullary cavity and/or region varies but most share a small (Wijk06-102 [Fig. 7A, B], IGWH 5, Wijk06-14, Wijk08-150, Wijk07-137) to moderately sized medullary cavity (TWE 4800075, Wijk10-520, Wijk fe II, TWE 4800085, Wijk06-636, Wijk07-3 [Suppl. Fig. S4E, F], IGWH 24 [Suppl. Fig. S5E, F], IGWH 21), the latter is the result of the expansion of the endosteal domain (i.e. erosion). MHI 1382b has a moderately to large sized medullary region that is nearly filled by endosteal bone. In TWE 48000074 the small medullary cavity is also nearly filled by endosteal bone. MHI 1382a (Suppl. Fig. S4C, D) and SMNS 55423, both show a small to moderately sized medullary region that is surrounded by endosteal bone. IGWH 2 displays a small medullary region made of endosteal bone and a large amount of calcified cartilage, which is surrounded by large erosion cavities (Suppl. Fig. S1L). In Wijk05-10 (Suppl. Fig. S5G, H) a large medullary region that consists of cancellous endosteal bone encompasses a central free cavity. Bone compactness values range in the sample of Eosauropterygia indet. from 68% to 94% (Table 1).

The visible growth patterns in these femora is as variable as their microanatomy but can be roughly categorized as followed: TWE4800085, IGWH 2, and Wijk fe II show a juvenile tissue, which is divided by indistinct subcycles (Suppl. Fig. S5A, B). Wijk06-102 (Suppl. Fig. S4A, B), TWE4800075, Wijk06-636, Wijk07-3 (Suppl. Fig. S4E, F), Wijk07-137, and Wijk08-150 show juvenile tissue in the innermost cortex, which is followed by a higher organized and lower vascularized tissue that is stratified by indistinct subcycles and finally ends in a thick layer of avascular highly organized tissue in the outermost cortex. This might indicate an advanced ontogenetic stage (Suppl. Fig. S4E, F). Wijk10-520, IGWH 5, MHI 1382b, SMNS 55423, TWE 48000074, and IGWH 24 also have juvenile tissue in the inner cortex preserved. The following cortex is regularly stratified by distinct growth marks (Suppl. Fig. S5E, F). Wijk05-10 shows a similar growth pattern with regular appearing growth marks but in the inner is no juvenile tissue preserved (Suppl. Fig. S5G, H). MHI 1382a, Wijk06-14, and IGWH 21 do not show juvenile tissue in the innermost cortex but their cortex is regularly stratified by growth marks.

Wijk06-86 differs from the others because the innermost cortex shows two to three distinct annuli that are then followed by very fast-growing tissue throughout the rest of the cortex (Suppl. Fig. S5C, D).

Suppl. Table 1. Femora of Eosauropterygia histologically studied. Listed taxonomically and according to dorso-ventral length of cross section. For a detailed histological description see also Supplementary Text and Supplementary Figures S1-S5.
Abbreviations: bc, bone compactness; LAG, line of arrested growth; na, not applicable; nm, not measurable.

specimen	bone length/ circum. In cm	medullary cavity/region	bc	growth pattern	locality/ stratigraphic age
“*Proneustico-saurus*” *silesiacus*					
MGW Wr. 4438s	11.9/ 1.35	small/reduced medullary cavity surrounded by small medullary region	97.3%	inner tissue made of vascularized juvenile bone; widely avascular cortex regularly stratified by LAGs accompanied by multiple rest lines; no separation into zones and annuli identifiable	Gogolin/ Anisian (Lower Muschelkalk, Gogolin Formation)
aff *Neusticosaurus*					
IPGB R feI	1.9/ 0.13	medullary region filled by endosteal bone	89%	inner tissue made of vascularized juvenile bone; alternating sequence of zones and annuli	Kirchheim Ladinian (Grenzbonebed)
IPGB R feII	2.1/ 0.15	medullary region filled by endosteal bone	99%	inner tissue made of vascularized juvenile bone; alternating sequence of zones, annuli and LAGs	Kirchheim Ladinian (Grenzbonebed)
IPGB R feIII	1.8/ 0.16	medullary region filled by endosteal bone with some large erosion cavities	96.5	inner tissue made of vascularized juvenile bone; alternating sequence of zones, annuli and LAGs	Kirchheim Ladinian (Grenzbonebed)
IPGB R feIV	~2.6/ 0.18	medullary region filled by endosteal bone with some large erosion cavities	95.6%	inner tissue made of vascularized juvenile bone; alternating sequence of zones, annuli and LAGs	Kirchheim Ladinian (Grenzbonebed)
Anarosaurus heterodontus					
Wijk07-11	> 2.0/ 0.3	moderately sized medullary cavity	82%	distinct annulus in the outer cortex followed by fast growing tissue	Winterswijk/ Anisian (Lower Muschelkalk)
Wijk06-38 (Klein 2012)	3.85/ 0.31	moderately sized medullary cavity	79%	no distinct annual growth marks, only diffuse subcycles	Winterswijk/ Anisian (Lower Muschelkalk)

Wijk06-266 (Klein 2012)	3.81/ 0.31	moderately sized medullary cavity	83%	no distinct annual growth marks, only diffuse subcycles	Winterswijk/ Anisian (Lower Muschelkalk)
Wijk fe I	nm/ 0.32	small to moderately sized medullary cavity	87%	no distinct annual growth marks, only diffuse subcycles	Winterswijk/ Anisian (Lower Muschelkalk)
Wijk06-84	4.05/ 0.39	small moderately sized medullary cavity	75%	no distinct annual growth marks, only diffuse subcycles	Winterswijk/ Anisian (Lower Muschelkalk)
Wijk09-582 (Klein 2012)	4.8/ 0.44	small to moderately sized medullary cavity	87%	distinct annulus in the outer cortex followed by fast growing tissue	Winterswijk/ Anisian (Lower Muschelkalk)
WijkA568	> 4.05/ 0.5	small to moderately sized medullary cavity	85%	no distinct annual growth marks, only diffuse subcycles	Winterswijk/ Anisian (Lower Muschelkalk)
Eosauropterygia indet.					
Wijk06-102	> 3.5/ 0.37	small medullary cavity	91%	juvenile tissue in the inner cortex; subcycles throughout cortex; thick layer of avascular highly organized tissue forms the outer cortex	Winterswijk/ Anisian (Lower Muschelkalk)
IGWH 2	4.5/ 0.38	moderately sized medullary region	86%	entire cortex is regularly stratified by distinct growth marks	Freyburg/ Anisian (Middle Muschelkalk)
TWE4800075	nm/ 0.42	large medullary cavity	na	juvenile tissue in the inner cortex; thick layer of avascular highly organized tissue forms the outer cortex	Winterswijk/ Anisian (Lower Muschelkalk)
Wijk10-520	nm/ 0.42	moderately sized medullary cavity	83%	juvenile tissue in the inner cortex; entire cortex is regularly stratified by distinct growth marks	Winterswijk/ Anisian (Lower Muschelkalk)
Wijk fe II	nm/ 0.43	small to moderately sized medullary cavity	84%	juvenile tissue in the inner cortex; subcycles throughout cortex	Winterswijk/ Anisian (Lower Muschelkalk)
Wijk06-86	> 2.3/ 0.44	moderately sized medullary cavity	83%	two distinct annuli in the inner cortex than very fast growing tissue in outer cortex	Winterswijk/ Anisian (Lower Muschelkalk)
IGWH 5	> 2.95/ 0.44	moderately sized medullary cavity	89%	juvenile tissue in the inner cortex;	Freyburg/ Anisian

				thick annulus forms the outer cortex	(Middle Muschelkalk)
TWE 48000085	nm/ 0.46	moderately sized medullary cavity	na	juvenile tissue with diffuse subcycles	Winterswijk/ Anisian (Lower Muschelkalk)
Wijk06-636	nm/ 0.47	moderately sized medullary cavity	85%	juvenile tissue in the inner cortex; thick layer of avascular highly organized tissue forms the outer cortex	Winterswijk/ Anisian (Lower Muschelkalk)
MHI 1382b	> 2.9/ 0.48	small medullary cavity	93%	juvenile tissue in the inner cortex; cortex regularly stratified by growth marks	Eigenrieden bei Mühlhausen/ (Middle Muschelkalk, mm orbicularis SS)
MHI 1382a	> 6.09/ 0.49	small medullary cavity	94%	no juvenile tissue!, entire cortex is regularly stratified by growth marks	Eigenrieden bei Mühlhausen/ (Middle Muschelkalk, mm orbicularis SS)
Wijk07-3	6.2/ 0.5	large medullary cavity	68%	juvenile tissue in the inner cortex; thick annulus forms the outer cortex	Winterswijk/ Anisian (Lower Muschelkalk)
Wijk06-14	> 3.4/ 0.5	small medullary cavity	75%	entire cortex is regularly stratified by growth marks	Winterswijk/ Anisian (Lower Muschelkalk)
TWE 48000074	nm/ 0.6	small/reduced medullary cavity	na	juvenile tissue in the innermost cortex, cortex is regularly stratified by growth marks, thick layer of highly organized tissue in the outer cortex	Winterswijk/ Anisian (Lower Muschelkalk)
Wijk08-150	6.8/ 0.6	small sized medullary cavity	86%	juvenile tissue in the inner and middle cortex; thick annulus forms the outer cortex	Winterswijk/ Anisian (Lower Muschelkalk)
Wijk07-137	nm/ 0.6	small sized medullary cavity	90%	juvenile tissue in the inner cortex; subcycles; thick layer of highly organized tissue forms the outer cortex	Winterswijk/ Anisian (Lower Muschelkalk)
SMNS 55423	9.54/ 0.8	reduced medullary cavity surrounded by small medullary region	90%	remains of juvenile tissue in the inner cortex, entire cortex is regularly stratified by growth marks	Kattowice/Anisian (Lower Muschelkalk /Gogolin Beds)
IGWH 24	> 4.9/ 0.85	moderately sized medullary cavity	83%	juvenile tissue in the inner cortex; regularly stratified	Freyburg/ Anisian

				by growth marks, thick layer of highly organized tissue forms the outer cortex	(Middle Muschelkalk)
Wjik05-10 not midshaft	9.3/ 0.9	large medullary region including small inner cavity	86%	entire cortex is regularly stratified by growth marks	Winterswijk/ Anisian (Lower Muschelkalk)
IGWH 21	> 7.7/ 0.95	moderately sized medullary cavity	87%	entire cortex is regularly stratified by growth marks	Freyburg/ Anisian (Middle Muschelkalk)
***Nothosaurus* spp.**					
SMNS 84844	> 13/ 0.9	large medullary region filled by endosteal bone	96%	diffuse growth marks throughout entire cortex	Crailsheim/ Ladinian (Grenzbonebed/Lower Keuper)
MHI 1113 ?not midshaft	>7.95/ 0.9	large spongious medullary region	84%	no growth mark record	unknown
SMNS 5308	> 13.8/ 1.1	large medullary region	93%	diffuse growth marks throughout entire cortex	Hohenecker Kalk/Ladinian (Upper Lettenkeuper)
SMNS Knapp 1869	14.56/ 1.1	large medullary cavity surrounded by cancellous structure	65%	regularly spaced annuli throughout remaining cortex	Roth am See/ Ladinian (Lettenkeuper)
IGPB R 54	16.5/ 1.2	moderately sized medullary cavity	78%	diffuse growth marks throughout entire cortex	Laineck, Bayreuth/ Anisian (Upper Muschelkalk)
SMNS 59373	9.31/ 1.4	reduced medullary cavity surrounded by moderately sized medullary region	85%	clear growth marks but not regularly spaced	Saarlouis A8/
MHI 1987	15.7/ 1.4	moderately sized medullary cavity	80%	clear growth marks but not regularly spaced	Ummenhofen/ Ladinian (Grenzbonebed/Lower Keuper)
MBR 960 ?not midshaft	>8.3/ 1.4	moderately sized medullary cavity surrounded by large medullary region	72%	regularly spaced annuli throughout remaining cortex	Bayreuth/ Anisian (Upper Muschelkalk)
SMNS 84856	> 7.5/ 1.41	small/reduced medullary cavity	93.3%	growth marks clearest in the outermost cortex	Crailsheim/ Ladinian (Grenzbonebed, Lower Keuper)
MHI 1992	19.3/ 1.5	small/reduced medullary cavity	94%	diffuse growth marks throughout entire cortex	Nitzenhausen/ Anisian (Upper Muschelkalk, mo2)
MHI 756	> 8.72/ 1.5	moderately sized medullary cavity surrounded by narrow cancellous structure	82%	clear growth marks but not regularly spaced	Bölgental/ Anisian (Upper Muschelkalk, m2-mo3)

MHI 279	> 8.45/ 1.6	large medullary cavity	67%	diffuse growth marks throughout entire cortex	Neidenfels I/ Ladinian (Upper Muschelkalk, m8, spinosus zone)
SMNS Nr. 79 Weismann	> 11.2/ 1.7	small medullary cavity surrounded by narrow cancellous structure	81%	regularly spaced annuli throughout entire cortex	Crailsheim/ Ladinian (?Upper Muschelkalk)
IGPB R 50	> 12/ 1.8	moderately sized medullary cavity	85%	regularly spaced annuli throughout entire cortex	Laineck, Bayreuth/ Anisian (Upper Muschelkalk)
MHI 2011 (compressed)	~28.5/ ~2	moderately sized medullary region	93%	clear growth marks but not regularly spaced	Dettelbach/ Ladinian (Upper Muschelkalk, m9a)
SMNS 81883 osteosclerotic	nm/ 2	large compact medullary region	na	clear growth marks but not regularly spaced	
SMNS 81886	nm/ 2	small medullary cavity surrounded by a wide cancellous structure	na	clear growth marks but not regularly spaced	
IGPB R 49 ?not midshaft	23/ 2.2	large medullary region	57.6%	regularly spaced annuli throughout entire cortex	Laineck, Bayreuth/ Anisian (Upper Muschelkalk)
MHI 1136	> 23/ 2.5	moderately sized medullary cavity surrounded by moderate medullary region	76%	clear and diffuse growth marks not regularly spaced	Wilhelmsglück/ Ladinian (Keuper, Ku1)

Supplementary Figures

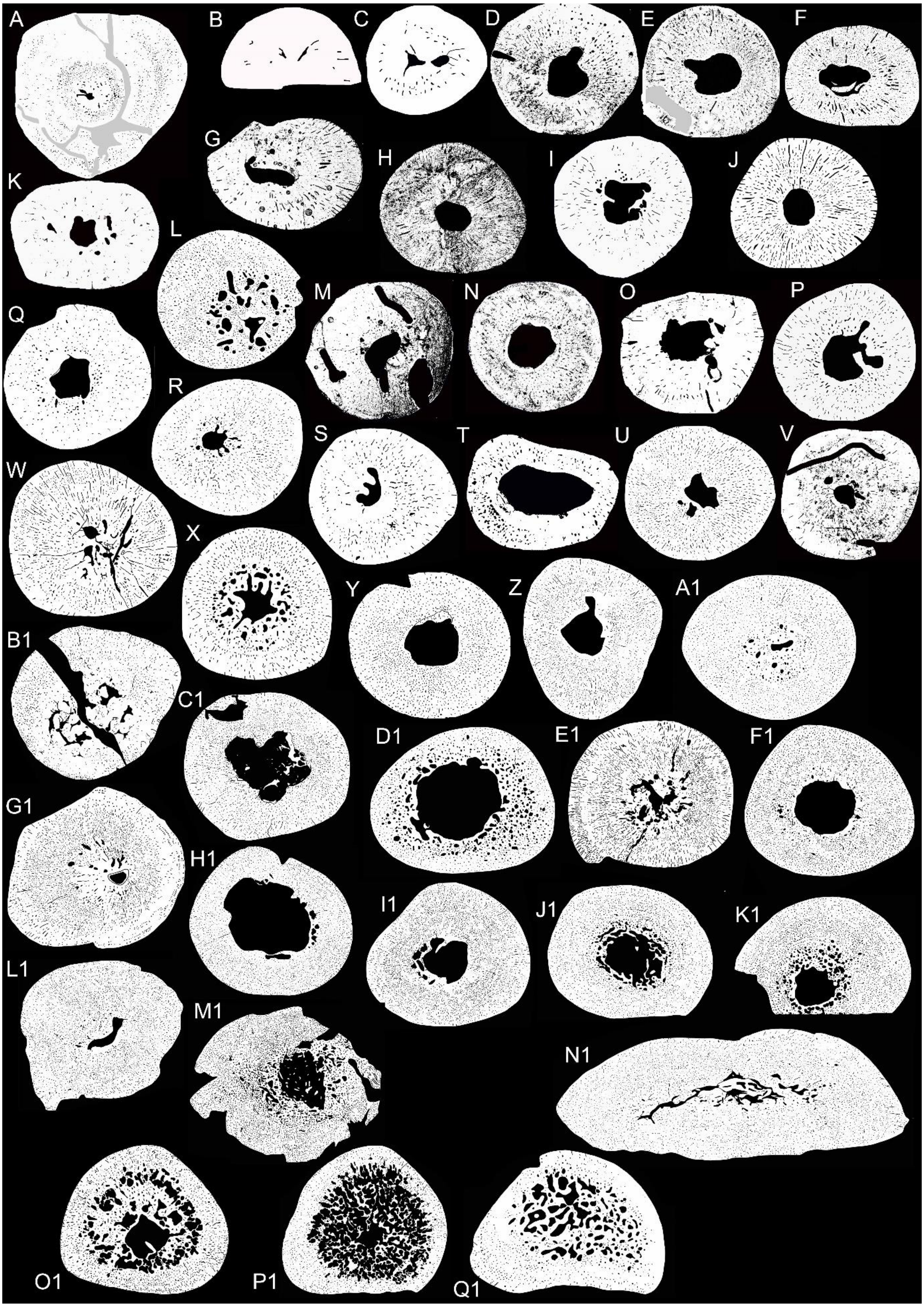

Suppl. Figure S1

Microanatomy of femora of *Proneusticosaurus silesiacus* (MGU Wr. 4438s), the pachypleurosaurs *Neusticosaurus* and *Anarosaurus*, the nothosaur *Nothosaurus* spp. and of several femora not to assign (Eosauropterygia indet.). All samples are listed according to table 1 but are not to scale. A-N1 are midshaft samples, O1-Q1 are samples from proximal or distal to midshaft. **A.** *Proneusticosaurus silesiacus* (MGU Wr. 4438s). **B.** aff. *Neusticosaurus* sp. (IPGB R fe2). **C.** aff. *Neusticosaurus* sp. (IPGB R fe4). **D.** *Anarosaurus heterodontus* (Wijk07-11). **E.** *Anarosaurus heterodontus* (Wijk06-38). **F.** *Anarosaurus heterodontus* (Wijk06-266). **G.** *Anarosaurus heterodontus* (Wijk0fe1). **H.** *Anarosaurus heterodontus* (Wijk06-84). **I.** *Anarosaurus heterodontus* (Wijk09-582). **J.** *Anarosaurus heterodontus* (WijkA-565). **K.** Eosauropterygia indet. (Wijk06-102). **L.** Eosauropterygia indet. (IGWH 2). **M.** Eosauropterygia indet. (Wijk0fe2). **N.** Eosauropterygia indet. (Wijk10-520). **O.** Eosauropterygia indet. (Wijk06-86). **P.** Eosauropterygia indet. (Wijk09-636). **Q.** Eosauropterygia indet. (IGWH 5). **R.** Eosauropterygia indet. (MHI 1382a). **S.** Eosauropterygia indet. (MHI 1382b). **T.** Eosauropterygia indet. (Wijk07-11). **U.** Eosauropterygia indet. (Wijk07-137). **V.** Eosauropterygia indet. (Wijk08-150). **W.** Eosauropterygia indet. (SMNS 55423). **X.** Eosauropterygia indet. (Wijk05-10). **Y.** Eosauropterygia indet. (IGWH 24). **Z.** Eosauropterygia indet. (IGWH 21). **A1.** Eosauropterygia indet. (SMNS 84844). **B1.** Eosauropterygia indet. (SMNS 5308). **C1.** Eosauropterygia indet. (IGPB R 54). **D1.** Eosauropterygia indet. (SMNS 1869). **E1.** Eosauropterygia indet. (SMNS 59373). **F1.** Eosauropterygia indet. (MHI 1987). **G1.** Eosauropterygia indet. (SMNS 84856). **H1.** Eosauropterygia indet. (MHI 279). **I1,** Eosauropterygia indet. (IGPB R 50). **J1.** Eosauropterygia indet. (MHI 756). **K1.** Eosauropterygia indet. (SMNS 79). **L1.** Eosauropterygia indet. (MHI 1992). **M1.** Eosauropterygia indet. (MHI 1136). **N1.** Eosauropterygia indet. (MHI 2011). **O1.**

Eosauropterygia indet. (MB R 960). **P1.** Eosauropterygia indet. (IPGB R 49). **Q1.** Eosauropterygia indet. (MHI 1113).

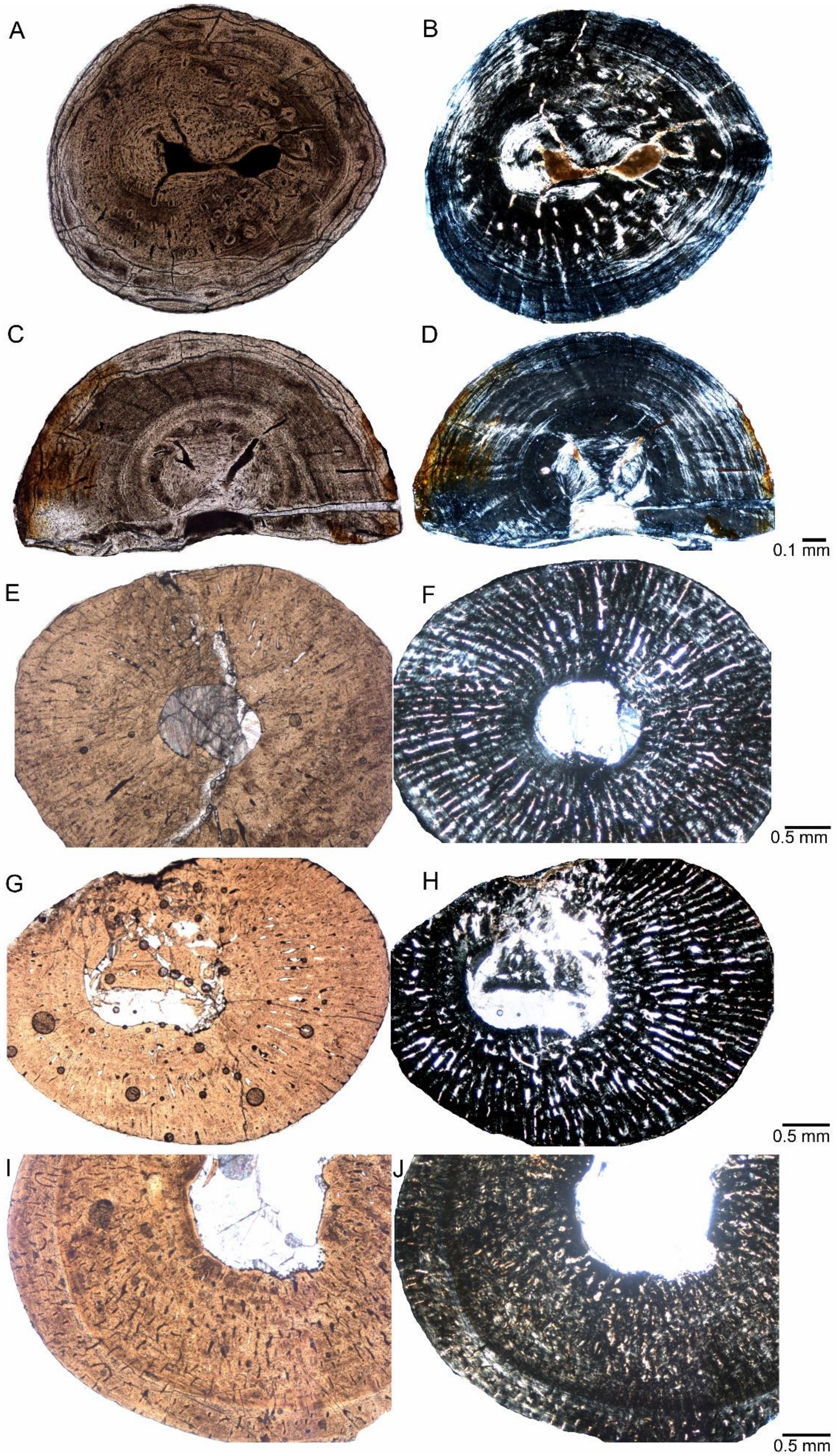
A
B
C
D
0.1 mm
E
F
0.5 mm
G
H
0.5 mm
I
J
0.5 mm

Suppl. Figure S2

Bone tissue, vascularization, and growth pattern in the pachypleurosaurs aff. *Neusticosaurus* from the Ladinian of Kirchheim and *Anarosaurus heterodontus* from the early late Anisian of Winterswijk. **A.** IGPB fe IV in normal and **B.** polarized light. Note the well vascularized and low organized parallel-fibred tissue in the inner half of the cortex (i.e. juvenile tissue) and the high organized lamellar bone in the outer cortex with numerous rest lines. **C.** IGPB fe II in normal and **D.** polarized light. Note the regularly high organized and low vascularized parallel-fibred tissue regularly stratified by growth marks. The medulla is here completely filled by endosteal bone. **E.** Wijk06-84 in normal and **F.** polarized light. Note the high vascular density by radial canals and the low organized parallel-fibred bone tissue. No growth marks are visible. **G.** Wijk0fe I in normal and **H.** polarized light. Note the high vascular density by radial canals and the low organized parallel-fibred bone tissue. No growth marks are visible. **I.** Wijk07-11 in normal and **J.** polarized light. Note the high vascular density by radial and longitudinal canals and the low organized parallel-fibred bone tissue. The outer cortex shows a distinct growth mark after which fast growth continues.

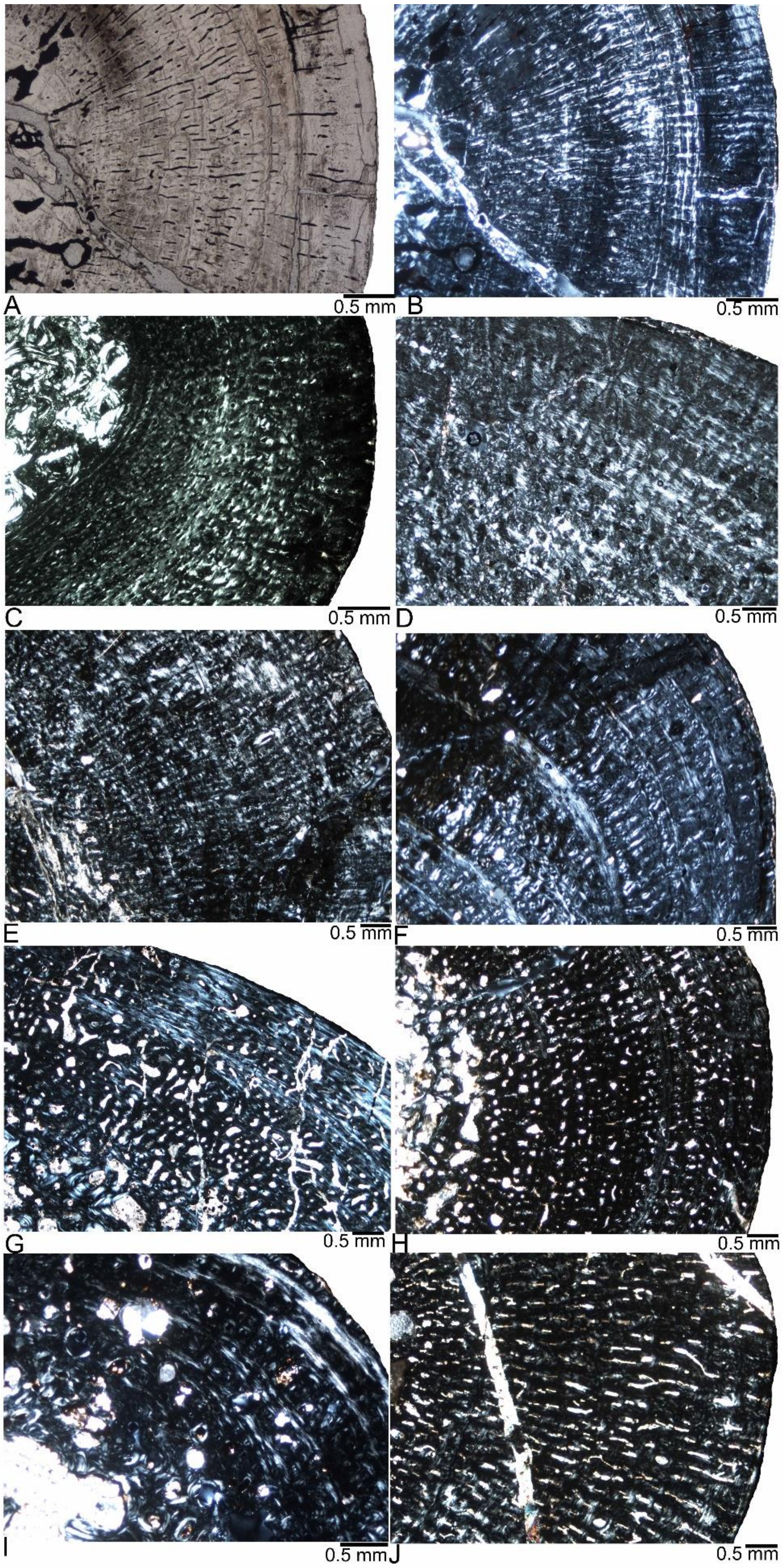
A
0.5 mm
B
0.5 mm
C
0.5 mm
D
0.5 mm
E
0.5 mm
F
0.5 mm
G
0.5 mm
H
0.5 mm
I
0.5 mm
J
0.5 mm

Suppl. Figure S3

Bone tissue, vascularization, and growth pattern in femora of large Nothosaurus spp. from the late Anisian and Ladinian of southern Germany. **A.** SMNS 59373 in normal and **B.** polarized light. Note the moderately vascularized parallel-fibred tissue with clear growth marks that are not regularly spaced. **C.** SMNS 84844 in polarized light, exhibiting moderately vascularized parallel-fibred tissue with only diffuse growth marks visible. **D.** MHI 1136 in polarized light, exhibiting moderately vascularized parallel-fibred tissue with only diffuse growth marks visible. **E.** MHI 1992 in polarized light exhibiting diffuse growth marks throughout the moderately vascularized cortex. **F.** SMNS Weismann 79 in polarized light displaying relatively regularly spaced annuli throughout entire cortex. A distinction into well vascularized zones, low to avascular annuli and LAGs is well visible. **G.** SMNS 81886 in polarized light showing a moderate vascular density, low organized parallel-fibred tissue with irregularly deposited growth marks and periosteal resorption. **H.** MHI 756 in polarized light showing irregularly deposited growth marks. **I.** SMNS Knapp 1869 in polarized light displaying regularly spaced growth marks in a low vascularized and high organized parallel-fibred tissue. **J.** MHI 279 in polarized light with highly vascularized and low organized parallel-fibred tissue depicting a distinct growth mark in the inner cortex but otherwise only diffuse growth marks.

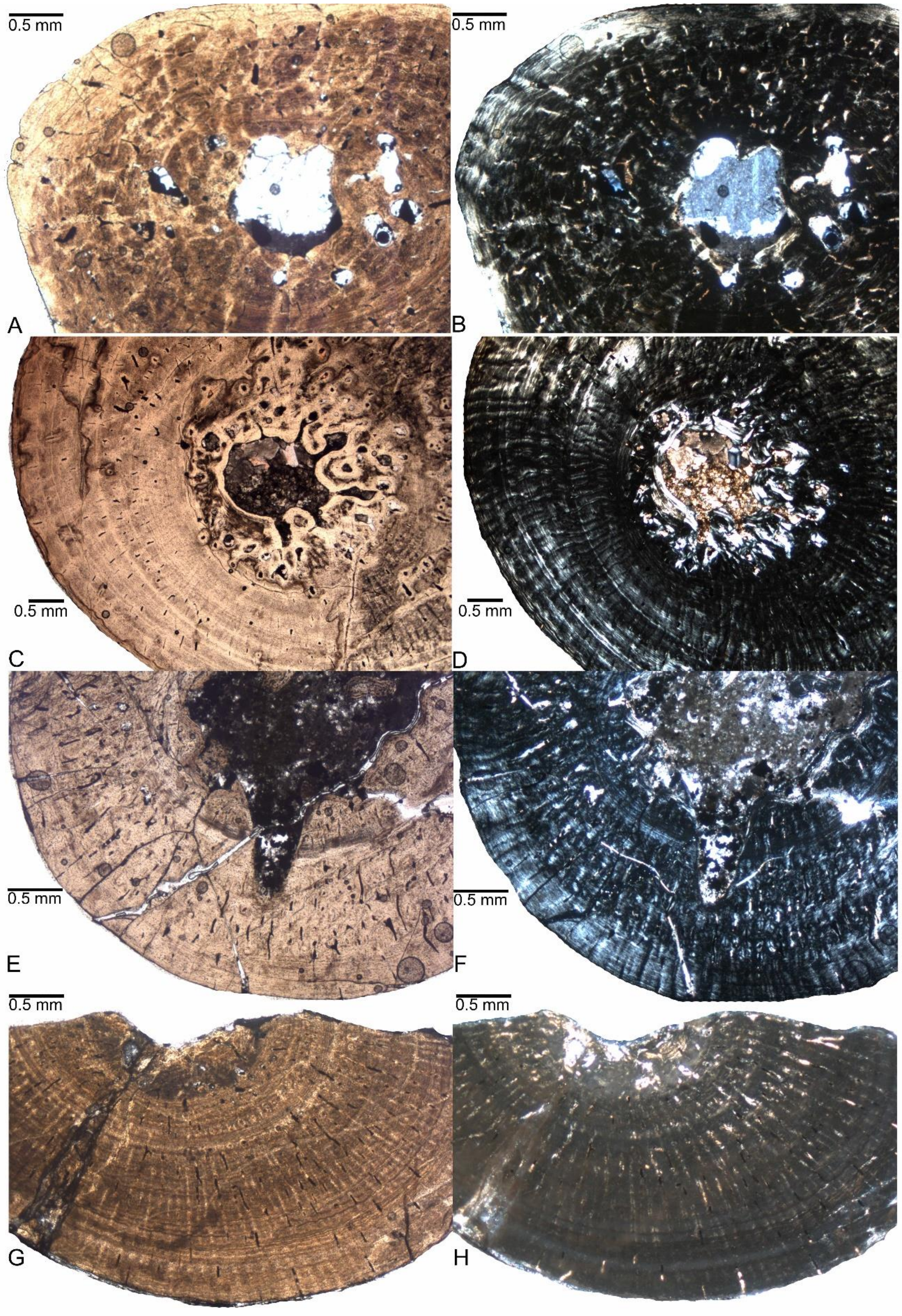
0.5 mm
0.5 mm
A
B
0.5 mm
0.5 mm
C
D
0.5 mm
0.5 mm
E
F
0.5 mm
0.5 mm
G
H

Suppl. Figure S4

Bone tissue, vascularization, and growth pattern in Eosauropterygia indet. femora (most likely referable to *Nothosaurus* sp.) from the early and middle Anisian. **A.** Wijk06-102 in normal and **B.** polarized light. Note the low vascularized but loosely organized parallel-fibred tissue and the thick layer of lamellar bone in the outer cortex. **C.** MHI 1382a in normal and **D.** polarized light. Note the low vascularized and high organized parallel-fibred tissue and the distinct growth marks. **E.** Wijk07-3 in normal and **F.** polarized light. Note the inner tissue which is less organized and higher vascularized when compared to the middle cortex and the thick layer of lamellar bone in the outermost cortex. **G.** Wijk06-14 in normal and **H.** polarized light. Note the low vascularized and high organized parallel-fibred tissue and the distinct growth marks.

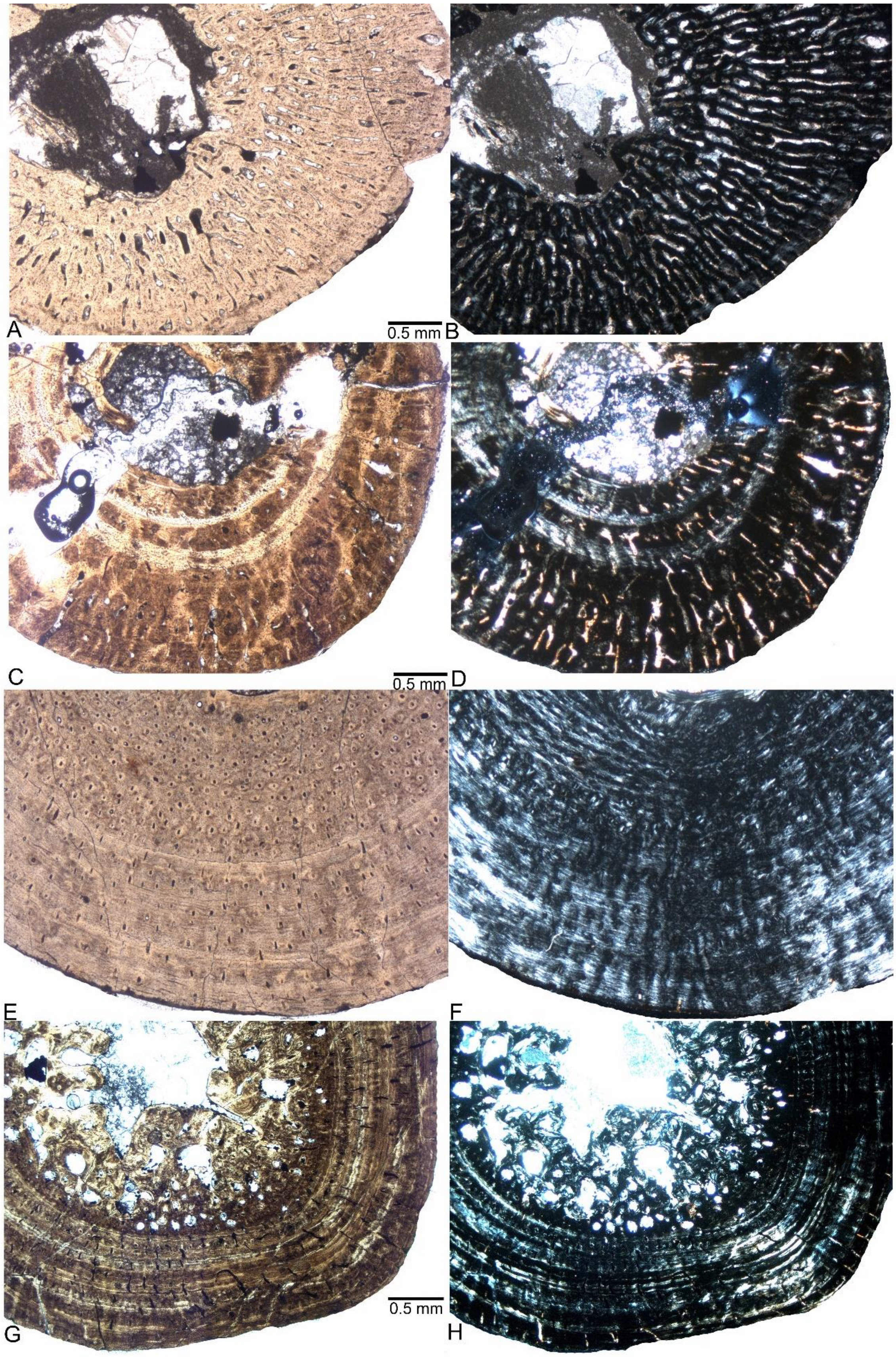
A
0.5 mm
B
C
0.5 mm
D
E
F
G
0.5 mm
H

Suppl. Figure S5

Bone tissue, vascularization, and growth pattern in Eosauropterygia indet. femora from the early and middle Anisian. **A.** TWE 48000085 (cf. ?*Cymatosaurus*) in normal and **B.** polarized light. Note the large radial vascular canals in a loosely organized parallel-fibred tissue. **C.** Wijk06-86 in normal and **D.** polarized light. Note the distinct annuli in the innermost cortex, which are followed by fast growing and well vascularized tissue. **E.** IGWH 24 in normal and **F.** polarized light. Note the high amount of longitudinal primary osteons in the inner cortex. **G.** Wijk05-10 in normal and **H.** polarized light. Note the regularly spaced growth marks and a high organized and moderately vascularized tissue.

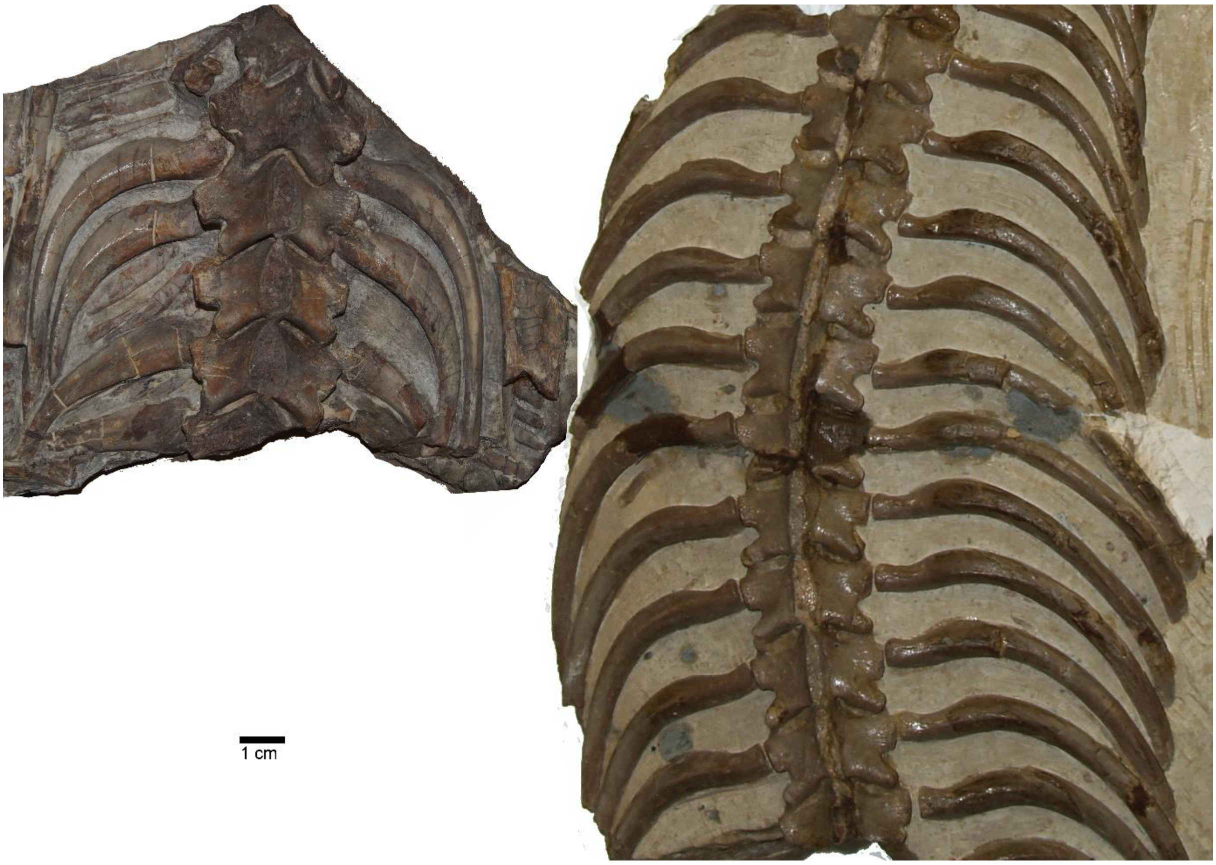

Suppl. Figure S6

Articulated vertebrae and ribs from the trunk region of *Nothosaurus* sp. from **A.** the Lower Muschelkalk of Gogolin (MGU Wr 3934s) and **B.** from the Lower Muschelkalk of Oberdorla (MB R 150). Note the differences in pachyostosis of proximal ribs and neural arches.

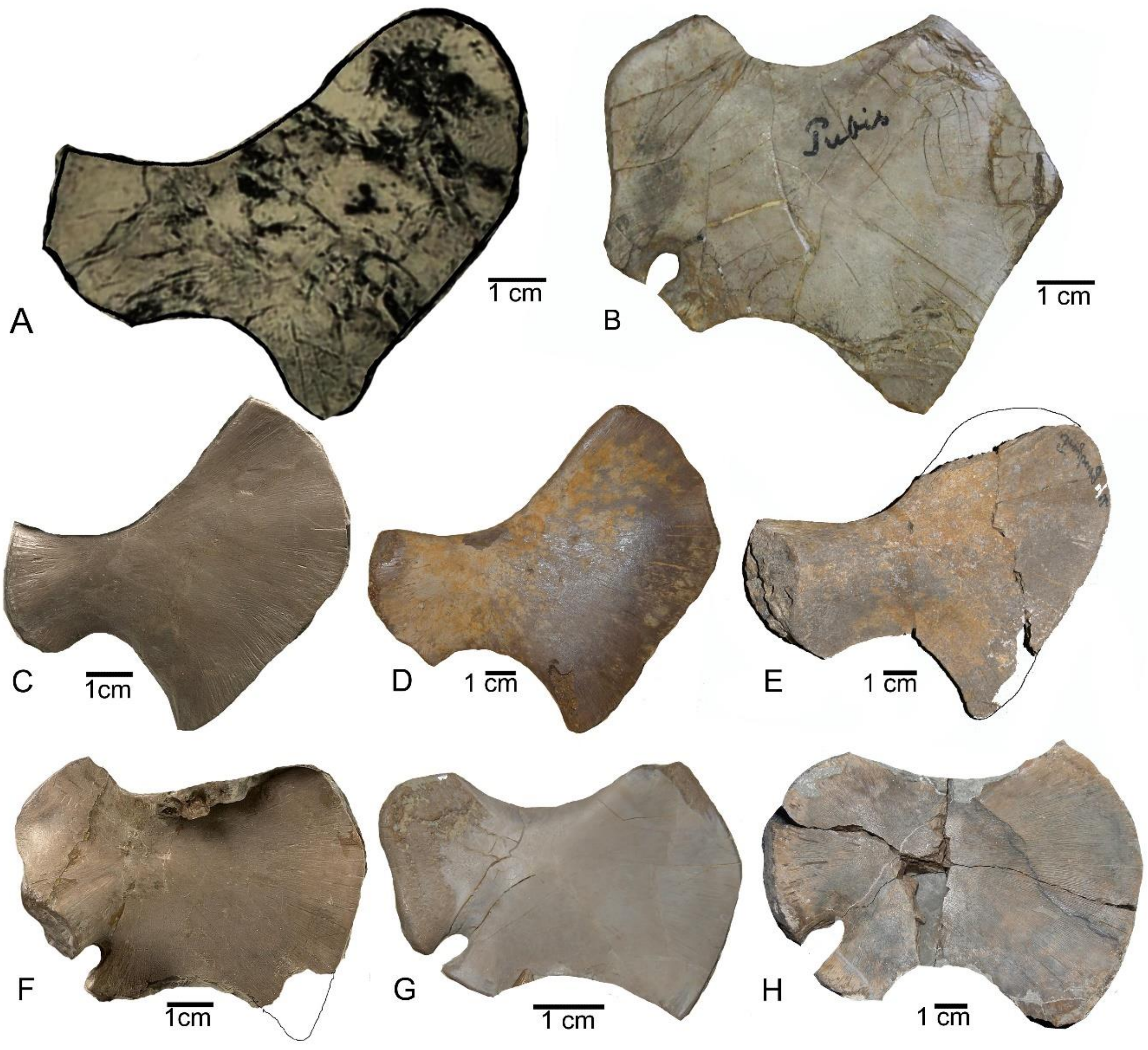

Suppl. Figure S7

Ischia and pubes of *Proneusticosaurus* from varies Lower Muschelkalk localities.

A. Ischium of *Proneusticosaurus* (modified from Volz 1902) from the early Anisian of Sacrau. Note the asymmetrical hatchet-shape of the posterior half, which is divided into a convex and straight margin. **B.** Pubis of *Proneusticosaurus* (MGU Wr. 4438s) from the early Anisian of Sacrau. Note the short/stout, nearly rectangular shape. **C.** Ischium from the early Anisian of Winterswijk (modified from Voeten et al. 2014), resembling the morphology of *Proneusticosaurus* (MGU Wr. 4438s). **D.** Ischium from the early Anisian of Rüdersdorf (MB R 259), resembling the morphology of *Proneusticosaurus* (MGU Wr. 4438s). **E.** Ischium from the early Anisian of Freyburg/Unstrut (IGWH uncatalogued), resembling the morphology of *Proneusticosaurus* (MGU Wr. 4438s). **F.** Pubis (modified from Voeten et al. 2014) from the early Anisian of Winterswijk in visceral view, resembling the morphology of *Proneusticosaurus* (MGU Wr. 4438s). **G.** Pubis from the early Anisian of Rüdersdorf (coll. EB), resembling the morphology of *Proneusticosaurus* (MGU Wr. 4438s). **H.** Pubis from the early Anisian of Freyburg/Unstrut (IGWH uncatalogued), resembling the morphology of *Proneusticosaurus* (MGU Wr. 4438s).